16th European Signal Processing Conference (EUSIPCO 2008), Lausanne, Switzerland, August 25-29, 2008, copyright by EURASIP

A SUBSPACE METHOD FOR DETECTION AND CLASSIFICATION OF RAIL DEFECTS

Zineb Mehel-Saidi[1], *Gérard Bloch*[1], *and Patrice Aknin*[2]

[1] Centre de Recherche en Automatique de Nancy (CRAN), Nancy–University, CNRS
CRAN-ESSTIN, Rue Jean Lamour, 54519 Vandoeuvre-les-Nancy Cedex, France
email: {zineb.mehel-saidi,gerard.bloch}@esstin.uhp-nancy.fr
[2] Institut National de Recherche sur les Transports et leur Sécurité (INRETS)
2 avenue Malleret-Joinville, 94114 Arcueil Cedex, France
email: aknin@inrets.fr

ABSTRACT

A non destructive evaluation system dedicated to rail inspection using a non-contact eddy current sensor embedded in a subway train is presented. An original processing approach borrowed from the MUSIC algorithm is proposed for rail surface defects detection and classification. This approach, based on the eigen decomposition of the signal covariance matrix, produces signal and noise subspaces. The projections of the typical defect signatures on the noise subspace and a multiplicative fusion of the elementary detectors are then performed. Compared to the approaches previously used in the same context, this approach yields to better results, particularly for shelling isolation. The proposed method has been tested successfully on the labeled defect data set of a subway line.

1. INTRODUCTION

Nondestructive testing (NDT) is used, amongst other fields, for rail monitoring of guided transportation systems. The goal is to ensure a high security level by detecting early rail breakages and to contribute to maintenance policies by localizing minor defects such as rail shelling. In this framework, the NDT techniques operate mainly from electromagnetic and/or ultrasonic signals, with various, and often combined, approaches [9, 16, 17, 12].

This study deals with the detection and classification of rail surface defects using a non-contact eddy current sensor embedded in a subway train, introduced in previous works [11]. Such a eddy current sensor is sensitive to any modification of the geometry and/or electromagnetic characteristics of the surface of a conductive target. In order to not only detect but also classify the rail defects (transverse splits, shellings,...) or singularities (fishplated joints, welded joints,...), the sensor has been associated with various techniques of classification [10, 3] or signal processing, such as a time heuristic approach, wavelet analysis, inverse filtering [1] and Independent Component Analysis (ICA) [2]. These methods are able to detect and classify fishplated joints and welded joints with high correct detection and low false detection rates, but cannot isolate correctly shellings.

An approach for rail monitoring, where eddy current measurements are processed by a subspace approach borrowed from the multiple signal classification (MUSIC) method, is presented here. This approach makes use of the fact that typical defect signatures can be highlighted. Originally, the MUSIC algorithm has been proposed to estimate the directions-of-arrival of multiple narrowband sources in passive sensor arrays [15, 6]. Then MUSIC has been used for ultrasonic non destructive evaluation applications [14], seismic wave separation [5], mobile communication [8, 7] and recently for buried object localization [13]. It is based on the eigenspace decomposition of the autocovariance matrix of the measured data in order to obtain signal and noise subspaces. The basic idea is then to project the typical signatures on the noise subspace resulting in a minimum value when the typical signature and the defect are close. The proposed approach gives satisfactory results and, contrary to the previously mentioned techniques proposed in this context, even for the isolation of shellings defects from the other rail singularities.

The organization of the paper is as follows. The instrumentation and signals are presented in Sec. 2. The high resolution MUSIC algorithm is briefly presented in its original form in Sect. 3. The application of this algorithm to simultaneously detect and classify the rail defects is presented in Sect 4. The results obtained by tuning the detectors from ROC curves are shown and discussed in Sec. 5.

2. SENSOR, SIGNALS, AND DEFECTS

The processed signals are provided by a non-contact double-coils and double-frequencies eddy current sensor embedded in a subway train, presented with more details in [11] and illustrated Fig. 1. The sensor has been designed and optimized

Figure 1: Eddy current sensor prototype.

according to the following specifications: positioning at 40 mm height, vertical and horizontal displacements of the sensor due to the bogie dynamics and 100 km/h maximum speed

of the train. Moreover, a particular attention has been given for strong acceleration levels (until 10g in subway context) and electromagnetic compatibility problem caused mainly by the traction currents that circulate in the rails.

The two differential coils ensure a greater immunity to the target-sensor distance variations for the detection of localized cracks as well as large shellings (see Fig. 2). The two supply frequencies make the sensor sensitive to the rail electromagnetic characteristics for different skin depths and give some relevant information for instance in the case of welded joint.

Figure 2: Example of shelling.

After preprocessing, eight real signals are available, which are the active and reactive parts of four complex channels corresponding to the two coils and the two frequencies of the sensor, as shown in Fig. 3. The device thus generates complementary information that will be aggregated during the phase of defect recognition. The digitalization is carried out with respect to the distance covered by the train with a fixed step of 5 mm. It must therefore be noted that, in all that follows, processed signals are discrete signals depending on the distance.

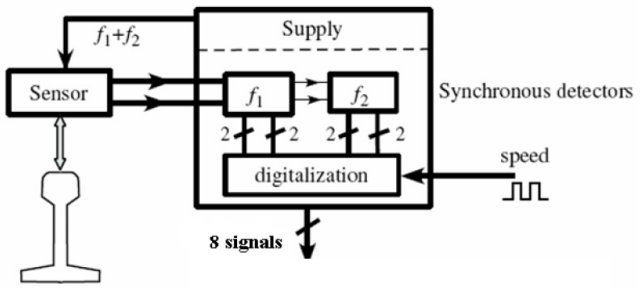

Figure 3: Data processing chain.

Fig. 4 gives an example of the first (active) signal on 500 m of rail. Particular points can be located, like switch (Sw), undulatory wear (UW) of the rail, fishplated joints (Fj), welded joints (Wj) and shellings (Sh). The complexity of the processing lies in the fact that the track presents a great number of singularities which must be distinguished from the real defects.

In order to reduce the impact of low dynamics of the inspection vehicle and the influence of electronic noise, a bandpass filtering between 0.05 m and 2.5 m is applied for the eight received signals. For the processing design and after perusal of records, track visits are required, in order to precisely label each detected singularity. For each of the 8 signals, a singularity is recorded as a vector of $n = 160$ samples (0.8 m), around the labeled point. This has led to gather 599 particular points distributed into three classes: fishplated joints (Fj), welded joints (Wj) and shellings (Sh). These particular points will be called defect in the following, even if only shellings are real defects.

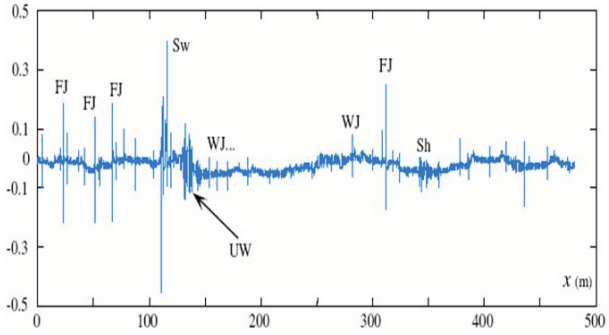

Figure 4: Example of raw signal evolution on 500 m track.

3. THE MUSIC ALGORITHM

The MUSIC (Multiple Signal Classification) algorithm has been initially proposed to process the signals received on an array of antennas and estimate the number of incident wavefronts and the emitter locations [15]. The basic data model used for characterizing the signals received on a array of m sensors is:

$$\mathbf{x} = \mathbf{E}\,\mathbf{a} + \mathbf{b}, \tag{1}$$

where $\mathbf{x}$ is the m-vector of received signals amplitudes, $\mathbf{a}$ the d-vector of incident signals amplitudes, $\mathbf{b}$ is a m-vector of white noise with zero mean and variance σ^2, and $\mathbf{E}$ is the $(m \times d)$-matrix of the signal arrival angles.

MUSIC is based on eigen decomposition of the received signal covariance matrix $\mathbf{R} = E[\mathbf{x}\mathbf{x}^H]$, where the subscript H denotes the conjugate transpose, giving:

$$\mathbf{R} = \mathbf{S}\,\mathbf{\Lambda}\,\mathbf{S}^H + \mathbf{B}\,[\sigma^2\mathbf{I}]\,\mathbf{B}^H, \tag{2}$$

where $\mathbf{S}$ is the signal subspace matrix and $\mathbf{B}$ is the noise subspace matrix. The projection operators onto the signal and the noise subspaces are given by:

$$\Pi_S = \mathbf{S}\,\mathbf{S}^H, \Pi_B = \mathbf{B}\,\mathbf{B}^H. \tag{3}$$

The so-called steering vector which represents the shape of the incident signals is considered as known. For example, in the case of planar wavefronts received on an array of sensors, the associated steering vector is given by: $\mathbf{e}(\theta) = \left[1,\ e^{-2j\pi f \frac{\delta \sin\theta}{c}},\ \ldots,\ e^{-2j\pi f(m-1)\frac{\delta \sin\theta}{c}}\right]^T$, where θ is the direction of arrival of the planar wavefronts, c is the velocity of the wawe), δ is the distance between two adjacent sensors, f is the signal frequency. The Euclidean distance $dist$ between the estimated noise subspace and the steering vector $\mathbf{e}(\theta)$ can be computed by: $dist^2 = \mathbf{e}(\theta)^H\,\Pi_B\,\mathbf{e}(\theta)$. Thus, the basic idea behind the MUSIC algorithm is that the maximum of $1/dist^2$ is obtained around the true signal arrival angles. Finally, the spatial spectrum obtained by the MUSIC algorithm is given by:

$$z(\theta) = \frac{1}{\mathbf{e}(\theta)^H\,\Pi_B\,\mathbf{e}(\theta)}. \tag{4}$$

4. PROPOSED METHOD

The proposed method involves three steps, described in the following subsections: building the defect typical signatures, deriving the elementary detectors from a signal moving window, enhancing the classification performances by fusion of the elementary detectors.

4.1 Typical signatures

As mentioned at the end of Sec. 2, the database of defect signatures, which are, for each of the 8 signals, vectors of $n = 160$ points (0.8 m), is distributed into 3 classes: fishplated joints (Fj), welded joints (Wj) and shellings (Sh). For each class $k \in \{1,2,3\}$, a "typical" signature $\mathbf{g}_{jk} = [g_{jk}(1,)\cdots,g_{jk}(n)]^T$ of length n can be obtained by averaging the corresponding signatures, scaled between -1 and +1, for each signal $j = 1,\ldots,8$. 132 (resp. 358, 109) defects are used to built the Fj (resp. Wj, Sh) typical signatures, shown resp. in Fig. 5, 6 and 7.

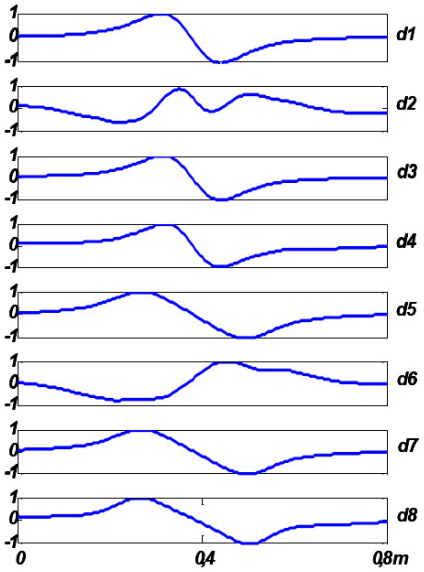

Figure 5: Typical signatures $\mathbf{g}_{j1}$ of the fishplated joints (Fj).

4.2 Elementary detectors

From the recorded signals, at each point for the design, but also later, at each instant for the detection and classification in real time, a sample $\mathbf{d}_j = [d_j(1),...,d_j(n)]^T$ is extracted from a window of length $n = 160$ samples, for each signal $j = 1,\ldots,8$. Note that the amplitudes of the Fj, Wj and Sh defects are different as shown in Fig. 4 and the proposed subspace approach is sensitive to the amplitude. Each sample is then normalized between -1 and 1 before any processing.

In case of defect, the defect typical signature gives the model of the current sample:

$$\mathbf{d}_j = \mathbf{g}_{jk} + \mathbf{b}_j, \tag{5}$$

where, for each signal j, $\mathbf{d}_j$, $\mathbf{g}_{jk}$ and $\mathbf{b}_j$ are the vectors of length n of resp. the moving window signal sample, the k-th typical signature and the white noise with variance σ_j^2.

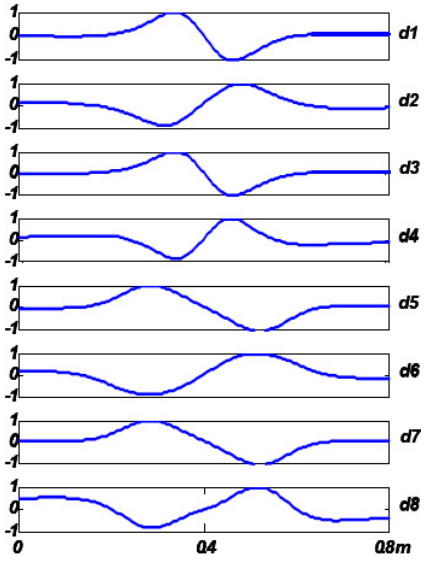

Figure 6: Typical signatures $\mathbf{g}_{j2}$ of the welded joints (Wj).

The eigen decomposition of the sample covariance estimate matrix $\mathbf{R}_j$ of the current sample $\mathbf{d}_j$ gives:

$$\mathbf{R}_j = \mathbf{S}_j \mathbf{\Lambda}_j \mathbf{S}_j^T + \mathbf{B}_j [\sigma_j^2 \mathbf{I}] \mathbf{B}_j^T, \tag{6}$$

where $\mathbf{S}_j$ and $\mathbf{B}_j$ are the signal and noise subspace matrices and the corresponding projection operators onto the signal and noise subspaces are given by:

$$\Pi_{S_j} = \mathbf{S}_j \mathbf{S}_j^T, \Pi_{B_j} = \mathbf{B}_j \mathbf{B}_j^T. \tag{7}$$

The Euclidean distance between the estimated noise subspace and a typical defect signature is minimal when this typical defect signature and the signal sample are close, or, for signal j and defect k, the detector:

$$z_{jk} = \frac{1}{\mathbf{g}_{jk}^T \Pi_{B_j} \mathbf{g}_{jk}} \tag{8}$$

is maximal.

4.3 Fusion of detectors

As shown in the diagram of Fig. 8, the defects are classified sequentially: the Fj defects first, then the Wj defects and finally the Sh defects.

For each defect k, eight detectors z_{jk} can be built by (8), from the active parts ($j = 1,3,5,7$) and reactive parts ($j = 2,4,6,8$) of the signals. Using this redundancy, given by the double-coils double-frequencies sensor, greatly improves the robustness of the detection. Thus two vectors achieving a multiplicative fusion of the elementary detectors are computed. The first vector, where the products involve the reactive parts:

$$\mathbf{c} = \left[\prod_{j=2,4,6,8} z_{j1}, \prod_{j=2,4,6,8} z_{j2}, \prod_{j=2,4,6,8} z_{j3} \right], \tag{9}$$

is used to differentiate the Fj defects ($k = 1$) from the Wj ($k = 2$) and Sh ($k = 3$) defects. The second, where the products

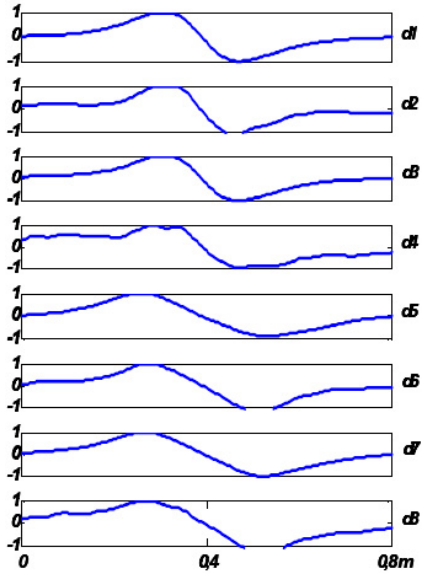

Figure 7: Typical signatures $\mathbf{g}_{j3}$ of the shellings (Sh).

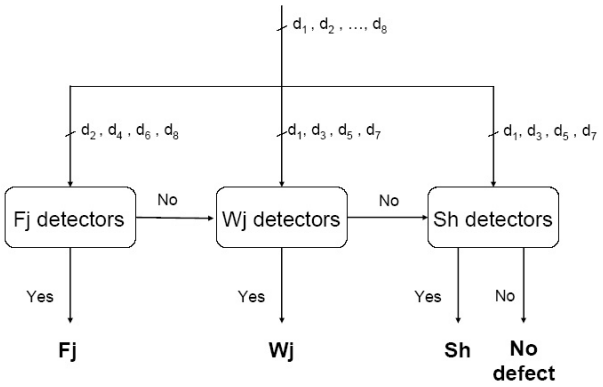

Figure 8: Diagram of detection and classification.

involve the active parts:

$$\mathbf{r} = \left[\prod_{j=1,3,5,7} z_{j2}, \prod_{j=1,3,5,7} z_{j3} \right], \qquad (10)$$

is used to differentiate the Wj ($k = 2$) defects from the Sh ($k = 3$) defects. The inclusion of the active or reactive parts of the signals is based on the Receiver Operating Characteristic (ROC) curves analysis, as presented in the next section.

Moreover, as the three typical signatures are very close to each other, the final detectors include amplitude tests of the original first signal window $\mathbf{d}_1$ without normalization:

$$\begin{aligned} d_{Fj} &= \{\max(\mathbf{c}) == \mathbf{c}(1)\} \text{ and } \{\max(\mathbf{d}_1) > Th_{Fj}\} \\ d_{Wj} &= \{\max(\mathbf{r}) == \mathbf{r}(1)\} \text{ and } \{\max \mathbf{d}_1) > Th_{Wj}\} \\ d_{Sh} &= \{\max(\mathbf{r}) == \mathbf{r}(2)\} \text{ and } \{\max(\mathbf{d}_1) < Th_{Sh}\}, \end{aligned} \qquad (11)$$

where Th_{Fj}, Th_{Wj} and Th_{Sh} are detection thresholds for Fishplated joints (Fj), Welded joints (Wj) and Shellings (Sh), respectively.

5. EXPERIMENTAL RESULTS

The choice of the signals involved in the detectors and the tuning of the thresholds are based on the analysis of the Receiver Operating Characteristic (ROC) curves. In such curves, the correct detection probabilities (Pc) are plotted with respect to the false detection probabilities (Pf); the nearest to the (0,1) point the ROC curve is, the better the tuning is.

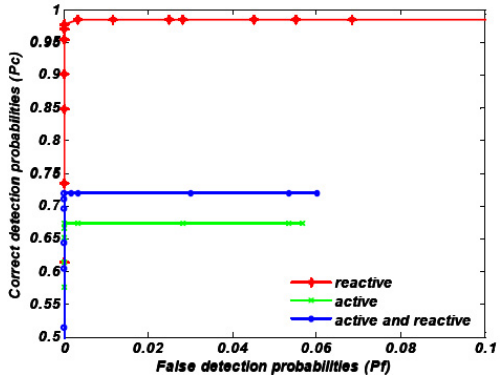

Figure 9: ROC curves for Fj.

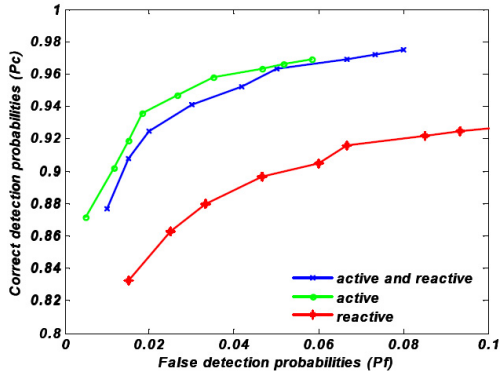

Figure 10: ROC curves for Wj.

For the defects Fj, Wj and Sh, Fig. 9, 10 and 11 present the ROC curves with $0.04 < Th_{Fj} < 0.16$, $0.013 < Th_{Wj} < 0.03$ and $0.013 < Th_{Sh} < 0.03$, where the probabilities are obtained by Leave One Out (LOO). This cross-validation procedure (see for instance [4]) involves splitting the data set of N examples into two parts: a learning set of $N-1$ samples and a validation set of only one example. The method iterates N times the classifier learning with, at each time, a different validation example. The probabilities can then be obtained by averaging the validation results. Applying LOO in our context involves simply to leave out one signature when computing the typical signatures. It can be seen from the figures that the reactive (resp. active) parts of the signals are better suited to test Fj (resp. Wj and Sh). The optimal tuning is obtained for $Th_{Fj} = 0.1$ (using only reactive parts), $Th_{Wj} = 0.019$ and $Th_{Sh} = 0.0272$ (using only active parts). The minimal distances to the (0,1) point are notably small: $d_{Fj} = 0.0155$, $d_{Wj} = 0.0546$ and $d_{Sh} = 0.0738$.

The detection and classification results, which simultaneously minimize the false alarm rate (Pf) and maximize the

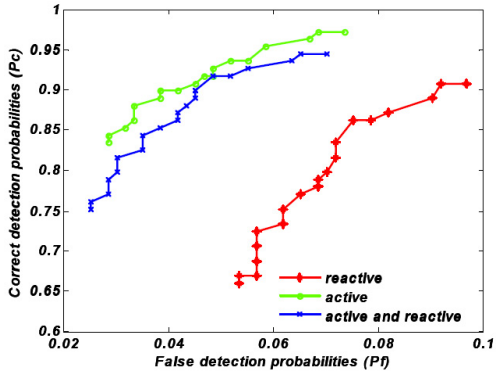

Figure 11: ROC curves for Sh.

correct detection rate (Pc), obtained by LOO, are given Table 1. The fishplated joints (Fj), welded joints (Wj), and even shellings (Sh) are detected and classified with very satisfying detection rates.

Defects	Pc	Pf
Fj	98.48%	0.33%
Wj	95.81%	3.51%
Sh	97.25%	6.84%

Table 1: Correct and false detection probabilities for each defect.

6. CONCLUSION

A non destructive evaluation system dedicated to rail inspection has been presented. An original processing approach borrowed from the MUSIC algorithm has been derived for rail surface defects detection and classification. This approach, based on the eigen decomposition of the signal covariance matrix, produces signal and noise subspaces. The projections of the typical defect signatures on the noise subspace and a multiplicative fusion of the elementary detectors are then performed. Compared to the approaches previously used in the same context, such as a time heuristic approach and the wavelet analysis ([1]), the proposed approach yields to better results, particularly for shelling isolation. Mixing and comparing the proposed approach with the ones previously used will be done and can still improve performance.

REFERENCES

[1] M. Bentoumi, P. Aknin, and G. Bloch, "On-line rail defect diagnosis with differential eddy current probes and specific detection processing," *Eur. Phys. J. AP*, vol. 23(3), pp. 227–233, Sept. 2003.

[2] M. Bentoumi, G. Bloch, P. Aknin, and G. Millerioux, "Blind Source Separation for detection and classification of rail surface defects," in *Studies in Applied Electromagnetics and Mechanics (SAEM)*, vol. 24 (9th Int. Workshop E'NDE, Saclay, France, May 15-16, 2003), pp. 112–119, Feb. 2004.

[3] M. Bentoumi, G. Millerioux, G. Bloch, L. Oukhellou, and P. Aknin, "Classification de Defauts de Rail par SVM," in *Proc. SCS'04*, Monastir, Tunisia, March 18-21. 2004, pp. 242–245.

[4] C. M. Bishop, *Pattern Recognition and Machine Learning*. Springer, 2006.

[5] S. Bourennane and A. Bendjama, "Higher order statistics for the seismic wave identification," in *Proc. Information, Communications and Signal Processing (ICICS), vol. 3*, Singapore, September 9-12. 1997, pp. 1372–1376.

[6] B. Friedlander, "A sensitivity analysis of MUSIC algorithm," *IEEE Trans. Acoust., Speech, Signal Processing*, vol. 38(10), pp. 1740-1751, Oct. 1990.

[7] L. C. Godara, "Application of Antenna Arrays to Mobile Communications, Part II: Beam-Forming and Direction-of-Arrival Considerations," *Proc. IEEE*, vol. 85(8), pp. 1195–1245, Aug. 1997.

[8] R. W. Klukas and M. Fattouche, "Radio signal direction finding in the urban radio environment," in *Proc. Nat. Tech. Meeting Institute Navigation*, San Francisco, CA. 1993, pp. 151160.

[9] F. Lanza di Scalea, P. Rizzo, S. Coccia, I. Bartoli, M. Fateh, E. Viola, and G. Pascale, "Non-contact ultrasonic inspection of rails and signal processing for automatic defect detection and classification," *Insight*, vol. 47(6), pp. 346–353, June 2005.

[10] F. Lauer, M. Bentoumi, G. Bloch, G. Millerioux, and P. Aknin, "Ho-Kashyap with Early Stopping vs Soft Margin SVM for Linear Classifiers - An Application," in *Lecture Notes in Computer Science*, vol. 3173 (Proc. ISNN 2004 Part I, Dalian, China, August 19-21), pp. 524–530, 2004.

[11] L. Oukhellou, P. Aknin, and J.-P. Perrin, "Dedicated sensor and classifier of rail head defects," *Control Eng. Practice*, vol. 7(1), pp. 57-61, Jan. 1999.

[12] P. Rizzo, I. Bartoli, M. Cammarata, and S. Coccia, "Rail: Digital signal processing for rail monitoring by means of ultrasonic guided waves," *Insight*, vol. 49(6), pp. 327–332, June 2007.

[13] Z. Saidi and S. Bourennane, "Cumulant-based coherent signal subspace method for bearing and range estimation," *EURASIP J Appl. Signal Process.*, vol. 2007, Article ID 84576, 2007.

[14] J. Saniie and X. M. Jin, "Spectral analysis for ultrasonic nondestructive evaluation applications using autoregressive, Prony, and multiple signal classification methods," *J. Acoust. Soc. Am.*, vol. 100(5), pp. 3165–3171, Nov. 1996.

[15] R.O. Schmidt, "Multiple emitter location and signal parameter estimation," *IEEE Trans. Antennas Propagat.*, vol. 34(3), pp. 276–280, March 1986.

[16] G. Zumpano G. and M. Meo, "A new damage detection technique based on wave propagation for rails," *Int. J. Solids Struct.*, vol. 43(5), pp. 1023–1046, March 2006.

[17] S. Yella, M. S. Dougherty, and N. K. A. Gupta, "Artificial intelligence techniques for the automatic interpretation of data from non-destructive testing," *Insight*, vol. 48(1), pp. 10–20, Jan. 2006.